Gene deletion of $P2Y_4$ receptor lowers exercise capacity and reduces myocardial hypertrophy with swimming exercise

Michael Horckmans, Elvira Léon-Gómez, Bernard Robaye, Jean-Luc Balligand, Jean-Marie Boeynaems, Chantal Dessy and Didier Communi

Am J Physiol Heart Circ Physiol 303:H835-H843, 2012. First published 3 August 2012;
doi: 10.1152/ajpheart.00256.2012

American Journal of Physiology - Heart and Circulatory Physiology publishes original investigations on the physiology of the heart, blood vessels, and lymphatics, including experimental and theoretical studies of cardiovascular function at all levels of organization ranging from the intact animal to the cellular, subcellular, and molecular levels. It is published 24 times a year (twice monthly) by the American Physiological Society, 9650 Rockville Pike, Bethesda MD 20814-3991. ESSN: 1522-1539. Visit our website at http://www.the-aps.org/.

Am J Physiol Heart Circ Physiol 303: H835–H843, 2012.
First published August 3, 2012; doi:10.1152/ajpheart.00256.2012.

Gene deletion of $P2Y_4$ receptor lowers exercise capacity and reduces myocardial hypertrophy with swimming exercise

Michael Horckmans,[1]* Elvira Léon-Gómez,* Bernard Robaye,[3] Jean-Luc Balligand,[2] Jean-Marie Boeynaems,[1,4] Chantal Dessy,* and Didier Communi[1]*

[1]*Institute of Interdisciplinary Research, Université Libre de Bruxelles, Brussels, Belgium;* [2]*Unit of Pharmacology and Therapeutics, Université catholique de Louvain, Brussels, Belgium;* [3]*Institute of Interdisciplinary Research, Université Libre de Bruxelles, Gosselies, Belgium; and* [4]*Department of Medical Chemistry, Erasme Hospital, Université Libre de Bruxelles, Brussels, Belgium*

Submitted 29 March 2012; accepted in final form 23 July 2012

Horckmans M, Léon-Gómez E, Robaye B, Balligand JL, Boeynaems JM, Dessy C, Communi D. Gene deletion of $P2Y_4$ receptor lowers exercise capacity and reduces myocardial hypertrophy with swimming exercise. *Am J Physiol Heart Circ Physiol* 303: H835–H843, 2012. First published August 3, 2012; doi:10.1152/ajpheart.00256.2012.—Nucleotides released within the heart under pathological conditions can be involved in cardioprotection or cardiac fibrosis through the activation purinergic $P2Y_2$ and $P2Y_6$ receptors, respectively. We previously demonstrated that adult $P2Y_4$-null mice display a microcardia phenotype related to a cardiac angiogenic defect. To evaluate the functional consequences of this defect, we performed here a combination of cardiac monitoring and exercise tests. We investigated the exercise capacity of $P2Y_4$ wild-type and $P2Y_4$-null mice in forced swimming and running tests. Analysis of their stress, locomotion, and resignation was realized in open field, black and white box, and tail suspension experiments. Exercise-induced cardiac hypertrophy was evaluated after repeated and prolonged exercise in $P2Y_4$ wild-type and $P2Y_4$-null hearts. We showed that $P2Y_4$-null mice have a lower exercise capacity in both swimming and treadmill tests. This was not related to decreased motivation or increased stress, since open field, white and black box, and mouse tail suspension tests gave comparable results in $P2Y_4$ wild-type and $P2Y_4$-null mice. Heart rate and blood pressure rose normally in $P2Y_4$-null swimming mice equipped with a telemetric implant. On the contrary, we observed a delayed recovery of postexercise blood pressure after exercise in $P2Y_4$-null mice. The heart rate increment in response to catecholamines was also similar in $P2Y_4$ wild-type and $P2Y_4$-null implanted mice, which is consistent with a similar level of cardiac β-receptor expression. Interestingly, the heart of $P2Y_4$-null mice displayed a reduced sympathetic innervation associated with a decreased norepinephrine level. We also demonstrated that exercise-induced cardiac hypertrophy was lower in $P2Y_4$-null mice after repeated and prolonged exercise. This was associated with a lower increase in cardiomyocyte size and microvessel density. In conclusion, besides its role in cardiac development, $P2Y_4$ receptor could constitute an important regulator of acute and chronic response to exercise.

extracellular nucleotides; exercise capacity; P2Y receptors; cardiac hypertrophy

EXTRACELLULAR NUCLEOTIDES were reported to be implicated in the protection of cardiomyocytes from hypoxic stress (29). UTP administration to rats reduced infarct size and enhanced myocardial function (28). The involvement of purinergic $P2Y_2$ receptors in the UTP-mediated cardioprotection in vivo has been recently demonstrated (6). Important amounts of extracellular nucleotides are secreted within the heart, especially under ischemia (9) or pressure overload (18). Furthermore, ATP and its degradation products were reported to participate to a negative feedback mechanism matching coronary blood flow to myocardial oxygen consumption during exercise (10).

Diverse actions of extracellular nucleotides acting at both ionotropic P2X receptors and G protein-coupled P2Y receptors have been described in many cell types (1). The human $P2Y_4$ receptor is a UTP receptor coupled to the phosphoinositide/Ca^{2+} pathway, encoded by a gene located on chromosome X and displaying a very restricted tissue distribution (7). The murine ortholog of human $P2Y_4$ receptor is activated by UTP and ATP (4, 15, 26), as described for the ubiquitously expressed mouse $P2Y_2$ receptor (16). Interestingly, $P2Y_2$ and $P2Y_4$ receptors were abundantly detected in the rat developing heart (5). $P2Y_4$-null mice have been generated in our laboratory (21) and display a microcardia phenotype (11). This was explained by a decreased heart weight increase during early postnatal development resulting from an angiogenic defect related to the expression of $P2Y_4$ on cardiac microvascular endothelial cells (11).

Here we demonstrate that $P2Y_4$-deficient mice display lower exercise capacity and a reduced effort-induced adaptive cardiac hypertrophy.

MATERIALS AND METHODS

Ethics Statement

All animal work has conducted according to relevant national and international guidelines and approved by the Ethics Committee of the Free University of Brussels.

Animals and Drugs

$P2Y_4^{0/+}$ and $P2Y_4^{0/-}$ CD1/C57Bl6 male mice were generated in our institute as described (14). Anti-CD31 (platelet endothelial cell adhesion molecule-1) and the rat isotype IgG2 antibodies were purchased from BD Biosciences (Le Pont-de-Claix, France). Anti-troponine was from Abcam (Cambridge, UK). The secondary antibodies were from Jackson ImmunoResearch (Suffolk, UK). Paraformaldehyde and paraffin were from Merck Eurolab (Strasbourg, France).

Exercise Capacity of $P2Y_4^{0/+}$ and $P2Y_4^{0/-}$ Mice

Swimming tests without cardiac monitorin. A 4-liter beaker filled with water was used to assess the exercise tolerance of mice (20). Briefly, a weight (2.5% of their body weight) was attached to the tail

* M. Horckmans and E. Léon-Gómez contribute equally to the work, and C. Dessy and D. Communi contribute equally to the work.

Address for reprint requests and other correspondence: D. Communi, Institute of Interdisciplinary Research (IRIBHM), ULB, Bldg. C (5th floor), Campus Erasme, 808 Route de Lennik, 1070 Brussels, Belgium (e-mail: communid@ulb.ac.be).

of the mice, and they were placed in the water and their behavior was observed. Swim-trained mice were then placed in the water. The time at which the mouse was unable to maintain buoyancy was recorded, and it was immediately removed from the beaker. For the experiments with repeated swimming tests, a 10-liter beaker was used as a swimming pool to assess the exercise adaptation of male mice. Swim-trained mice were placed in the water during 90 min, twice a day. After 3 wk, the animals were euthanized and the hearts collected for further analysis.

Motorized treadmill. Individual mice were placed on a motorized treadmill with a mild motivational shock bar (Eco-6M Treadmill; Columbus Instruments, Columbus, OH). Exercise capacity was quantified by the number of breaks during 5 min at a speed of 13 or 16 m/min.

Stress and Locomotion Tests

Open field experiments. $P2Y_4^{0/+}$ and $P2Y_4^{0/-}$ mice were placed in a 40 × 40 cm field surrounded by wall under dim light (15 lux). Activity was measured for 30 min to assess total distance traveled, the time spent in the central zone (area > 10 cm from walls), the latency to enter in zone, and the frequency in zone. Activity during the open field was recorded and videotaped via an overhead camera. Open field data were automatically analyzed by a computer-operated tracking system (Noldus Information Technology). The test was performed on 20 mice from each group.

Black and white box test. In the black and white two-compartment box used here, an opening was located centrally at floor level, connected the both compartments. A dark box was painted black and covered with a lid. The other box (not covered) was painted white and lit by a light (400 lx). At the start of the session, the mice were placed in the white compartment, head facing a corner. The time spent in the lit box was noted during the 10-min period of the test. A camera located above the test box was used to observe the animal. The data were automatically analyzed by a computer-operated tracking system (Noldus Information Technology). The test was performed on 20 mice from each group.

Tail suspension test. The mouse was hung on the hook by an adhesive tape placed 20 mm from the extremity of its tail, and it was kept away from the nearest object. The time before immobility periods (time before resignation) and the number of movements were measured by an observer in a blinded fashion. Each mouse was used only once for each experimental session.

Swimming Tests with Cardiac Monitoring

Implants were surgically inserted as follows: under anesthesia with a mixture of ketamine (100 mg/kg) and xylazine (10 mg/kg), animals were kept on a heating pad throughout implantation of the blood pressure (BP) telemeter (model TA11PA-C10, Sciences International, St. Paul, MN). The left common carotid artery was isolated, and the tip of the catheter was retrogradely inserted into the aorta until the aortic arch. The catheter was connected to the body of the implant, placed in a subcutaneous pouch in the right flank. When mice had recovered from the anesthesia, they were housed in individual cages placed on top of the telemetric receivers in a light-dark cycled recording room. Mice were fed with Scientific Animal Food Engineering and water ad libitum.

After surgery recovery, mice were trained during 3 days in a 26 × 20 × 14 cm swimming pool starting from 5, 7, and 10 min at 35°C. Recordings were obtained during the morning when the mice were generally quiet. Each session included a 30-min recording of resting pressure, 10 min of exercise, and 20 min of recovery. To obtain pressure and heart rate (HR) values during the resting period, mice were kept in theirs cage and continuous recordings of 24 h were performed, and online recordings were digitized (range, 20 to 2,000 Hz) and stored for further analysis. Relatively low resting HR (around 500 beats/min) were indicative of full recovery and resting state. For each mouse, two recording were done in separate days.

BP signals (and HR, derived from pressure waves) from the aortic arch were measured in conscious, unrestrained animals with surgically implanted, miniaturized telemetry devices. The investigation conforms with the Guide for the Care and Use of Laboratory Animals published by the National Institutes of Health (NIH Publication No. 85-23, Revised 1996).

The telemetered BP signal obtained after the magnetic activation of the probe was generated as a calibrated analog signal (UA10; DSI, St. Paul, MN). Spectral analysis using a fast Fourier transformation algorithm on sequences of 512 points was performed using the HEM 3.4 software (Notocord Systems) on systolic BP (SBP) and HR recordings. The total spectral area was examined in each mouse. The area under the curve was calculated for frequencies below 0.05 and 0.05–0.4 Hz and above 0.4 up to 5 Hz. Values were then examined for statistical changes between wild-type (WT) and knockout (KO) mice as previously described (8).

Catecholamine Response in $P2Y_4^{0/+}$- and $P2Y_4^{0/-}$-Implanted Mice

Implanted mice were injected with dobutamine (20 μg/g) plus atropine (1 μg/g). The recording of HR was performed 5, 10, 60, and 120 min after injection. Online recordings were digitized (range, 20 to 2,000 Hz) and stored for further analysis. HR was measured in conscious, unrestrained animals with surgically implanted, miniaturized telemetry devices. The telemeter signal obtained after the magnetic activation of the probe was generated as a calibrated analog signal (UA10; DSI, St. Paul, MN). Values were then examined for statistical changes between control and treated mice.

Adrenergic Receptor Quantification in $P2Y_4^{0/+}$ and $P2Y_4^{0/-}$ Hearts

Total RNAs were extracted using TRIzol reagent (Life Technologies, Groningen, The Netherlands) and RNeasy kit column (Qiagen, Hilden, Germany) from total heart of $P2Y_4^{0/+}$ and $P2Y_4^{0/-}$ mice. RNA was reverse transcribed using Superscript II Reverse Transcriptase. Quantitative PCR were performed using specific primers for adrenergic receptors (α_{1a}, α_{1b}, α_{1d}, α_{2a}, α_{2b}, α_{2c}, β_1, β_2, and β_3). Control genes were selected for their stability after analysis using Genorm program. Ribosomal protein L13 (RPL13) and hypoxanthine phosphoribosyltransferase (HPRT) specific primers were selected using Primer Express 2.0 software and specific parameters. RT-PCR amplification mixtures contained 2 ng template cDNA. Reactions were run on a 7,500 Fast Real-Time PCR System (Applied Biosystems). Means ± SE of normalized ratios were obtained using qBase software. Each assay was performed in duplicate for at least two independent preparations of heart. PCR data were normalized for each gene to RPL13 and HPRT housekeeping genes.

Catecholamine Quantification in $P2Y_4^{0/+}$ and $P2Y_4^{0/-}$ Mice

Cardiac catecholamine measurements. Hearts of $P2Y_4^{0/+}$ and $P2Y_4^{0/-}$ 12-wk-old mice were harvested and homogenized in 0.01 N HCl and 1 mM EDTA at 0°C. The supernatant was used to quantify norepinephrine, epinephrine, and dopamine levels, using 3-CAT research ELISA (Labor diagnostika nord), which were normalized to heart weight.

Urine catecholamine measurements. After five days of acclimatization, mice were kept in metabolic cages 24 h for determining urinary levels of dopamine, epinephrine, and norepinephrine and normalized with the level of creatinine. Water and food were allowed ad libitum. After urine collection from $P2Y_4^{0/+}$ and $P2Y_4^{0/-}$ mice, creatinine was quantified by the Jaffé method, whereas the concentrations of dopamine, epinephrine, and norepinephrine were measured by HPLC with electrochemical detection.

Quantification of Sympathetic Nerve Fibers in P2Y$_4^{0/+}$ and P2Y$_4^{0/-}$ Hearts

For the quantification of sympathetic nerve fibers, analysis of immunofluorescent staining was performed on left ventricular posterior wall. Heart of seven P2Y$_4^{0/+}$ and seven P2Y$_4^{0/-}$ mice were sectioned at a thickness of 7 μm. Tissues were incubated with anti-tyrosine hydroxylase (1:200 dilution; Abcam) in 1% horse serum and 0.1% Triton in PBS overnight at 4°C. Texas red-conjugated anti-sheep IgG from donkey was used as secondary antibody for the tyrosine hydroxylase staining. The surface labeled with the antibody against tyrosine hydroxylase was measured using ImageJ software. The labeled nerve fibers was qualitatively estimated from 10 randomly selected fields and expressed as the ratio of labeled nerve fiber area to total area.

Cold Challenge Experiments

Mice were single caged and transferred to a 4°C environment for 3 h. The colonic temperature was measured as an indication of core body temperature at 0, 30, 60, 120, and 180 min, respectively. A lubricated thermistor probe was inserted 2 cm into the rectum and held in place until a stabilized measurement was achieved. An average of three measurements was taken from each mouse at indicated time points.

Immunohistochemical Analysis in Cardiac Hypertrophy Experiments

After cervical dislocation, hearts were harvested, weighed, and frozen directly in optimum cutting temperature compound (VWR Scientific). Heart sections (7 μm) were fixed with methanol and stained with hematoxylin-eosin, 4,6-diamidino-2-phenylindole, and antibodies against CD31 or troponin. Microvessel and cardiomyocyte densities were quantified in complete transversal cross sections by examining 15 fields per section covering at least 40% of each tested heart, at ×20 magnification, in a blinded fashion. To quantify cardiomyocyte size, microscope lighting, focus, and field selection were optimized for distinction of cell boundaries. Fields were chosen to increase the probability of cardiomyocytes being visualized in appropriate cross section and not tangentially. Cardiomyocytes were outlined manually, and cardiomyocytes size was measured using ImageJ software.

Statistics

Data are expressed as means ± SE for in vitro and vivo studies. End-point comparisons with two groups were performed using an unpaired two-tailed Student's *t*-test (Prism Software, version 5; GraphPad). For parallel repeated-measures studies, two-way ANOVA was used with Bonferroni post hoc evaluations to determine the significance for individual time points (Prism Software; GraphPad). Data of HR and BP during exercise were analyzed using linear mixed-effect model to account for repeated measures (SPSS Statistics Software, IBM, Chicago, IL). For all studies, P values were considered as $^*P < 0.05$, $^{**}P < 0.01$, and $^{***}P < 0.001$.

RESULTS

Lower Exercise Capacity of P2Y$_4$-Deficient Mice

Swimming tests were performed using 12-wk-old P2Y$_4^{0/+}$ and P2Y$_4^{0/-}$ mice with a paper clip as light ballast (Fig. 1*A*). The time at which the mouse became unable to maintain complete buoyancy was defined as point of exhaustion, and this value was significantly lower for P2Y$_4^{0/-}$ mice: 15.6 ± 0.8 versus 25.6 ± 1.6 min for P2Y$_4^{0/+}$ mice (means ± SE; $N = 8$; $^{***}P < 0.001$; F ratio, 4.82) (Fig. 1*A*). To further evaluate the exercise tolerance of P2Y$_4$-deficient mice, we performed motorized treadmill tests with a mild motivational shock bar on 12-wk-old P2Y$_4^{0/+}$ and P2Y$_4^{0/-}$ mice (Fig. 1*B*). Exercise capacity was quantified by the number of breaks observed when the mouse stopped running and knocked the shock bar. Breaks were counted during 5 min at speeds of 13 or 16 m/min. As shown in Fig. 1*B*, there was a significant increase in break counts for P2Y$_4^{0/-}$ mice correlated with strong signs of tiredness.

Comparable Response to Stress in P2Y$_4^{0/+}$ and P2Y$_4^{0/-}$ Mice

To exclude the possibility that stress, depression, or motivational factors could affect the result of exercise tests, we performed open field, white and black box, and mouse tail suspension experiments. In the open field test, the total distance traveled was indicative of the general level of activity, whereas the percentage of time spent in the center of the field was used as an index of the anxiety state of mice. No significant discrepancy was observed between P2Y$_4^{0/+}$ and P2Y$_4^{0/-}$ mice in the total distance traveled, time before center entry, time in center area, and the number of center entries (Fig. 2*A*). The white and black box and tail suspension tests also revealed no discrepancy between P2Y$_4^{0/+}$ and P2Y$_4^{0/-}$ mice (Fig. 2, *B* and *C*).

Cardiac Monitoring of P2Y$_4^{0/+}$ and P2Y$_4^{0/-}$ Mice During Swimming Test

We decided to evaluate cardiac function during exercise by a cardiac monitoring of P2Y$_4^{0/+}$- and P2Y$_4^{0/-}$-swimming mice. Adult mice were chronically equipped with telemetry implants to measure HR and BP in awaked unrestrained conditions and during a short swimming exercise (Fig. 3). The data have been analyzed using linear mixed effects model (SPSS Statistics Software). The mean HR and BP measured over a 24-h period were

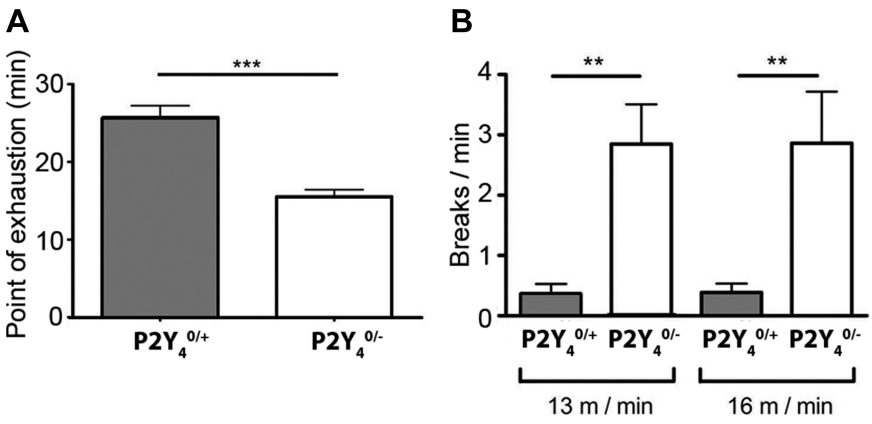

Fig. 1. Reduced exercise capacities of purinergic P2Y$_4$-null mice. *A*: tolerance of P2Y$_4^{0/+}$ and P2Y$_4^{0/-}$ mice to swimming test. A 4-liter beaker filled with water (25°C) was used as a swimming pool to assess the exercise tolerance of swim-trained P2Y$_4^{0/+}$ and P2Y$_4^{0/-}$ mice with a paper clip as light weight. The time at which the mouse was unable to maintain complete buoyancy was recorded. Results represent means ± SE for 8 P2Y$_4^{0/+}$ and 8 P2Y$_4^{0/-}$ mice ($^{***}P < 0.001$). *B*: reduced exercise capacity of P2Y$_4^{0/+}$ and P2Y$_4^{0/-}$ mice using motorized treadmill. Individual mice were placed on a motorized treadmill with a mild motivational shock bar. Exercise capacity was quantified by the number of breaks during 5 min at a speed of 13 or 16 m/min. Results represent means ± SE for 12 P2Y$_4^{0/+}$ and 12 P2Y$_4^{0/-}$ mice ($^{**}P < 0.01$).

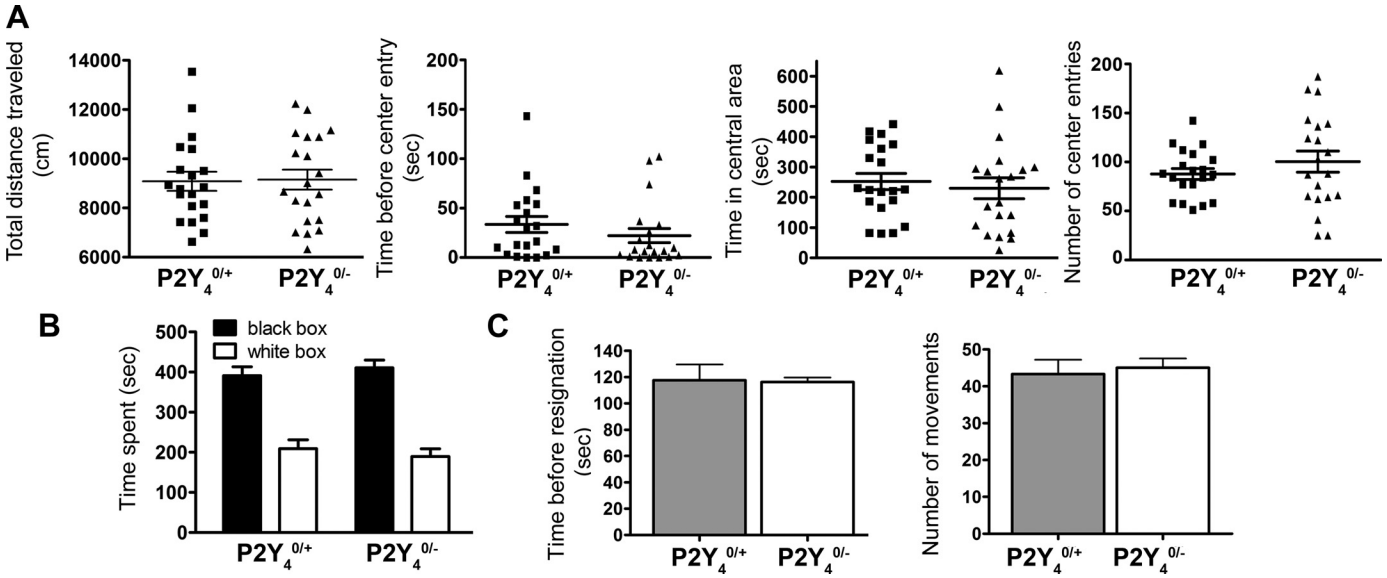

Fig. 2. Analysis of stress, locomotion, and resignation of $P2Y_4$ wild-type and $P2Y_4$-deficient mice. $P2Y_4^{0/+}$ and $P2Y_4^{0/-}$ mice were challenged into the open field (*A*), the black and white box (*B*), and tail suspension (*C*) tests to evaluate their locomotion capabilities and response to stress. All the results represent means ± SE for 20 $P2Y_4^{0/+}$ and 20 $P2Y_4^{0/-}$ mice. *A*: $P2Y_4^{0/+}$ and $P2Y_4^{0/-}$ mice were placed in a 40 × 40 cm field surrounded by wall under dim light. Activity was measured for 30 min to assess total distance traveled, the time spent in the central zone (area >10 cm from walls), the latency to enter in zone, and the frequency in zone. *B*: in the black and white two-compartment box, a dark box was painted black and covered with a lid, and the other box (not covered) was painted white and lit by a light. The time spent in the lit box was noted during the 10-min period of the test. *C*: the mouse was hung on the hook by an adhesive tape placed 20 mm from the extremity of its tail. The time before resignation and the number of movements were measured in a blinded fashion. Each mouse was used only once for each experimental session.

not significantly different between $P2Y_4^{0/-}$ and $P2Y_4^{0/+}$ mice (data not shown). During swimming, HR and SBP increased to the same extent in $P2Y_4$-null and WT mice (Fig. 3, *A* and *C*). Postexercise HR was not significantly different in $P2Y_4$-deficient mice (Fig. 3*B*). Interestingly, the postexercise BP recovery was significantly slower in $P2Y_4^{0/-}$ mice (Fig. 3, *C* and *D*), characterized by a change of 55 ± 22% in the ΔSBP, measured as the ratio between SBP 5 min after exercise and SBP during swimming.

Catecholamine Responsiveness, Catecholamine Level, and Adrenergic Receptor Expression in $P2Y_4$ WT and $P2Y_4$ KO Mice

Injection of dobutamine (20 μg/g) plus atropine (1 μg/g) was performed in $P2Y_4$ WT and $P2Y_4$ KO mice to evaluate maximal increase in HR (Fig. 4, *A* and *B*). As shown in Fig. 4*A*, a 10-min period of exercise (swimming) or dobutamine

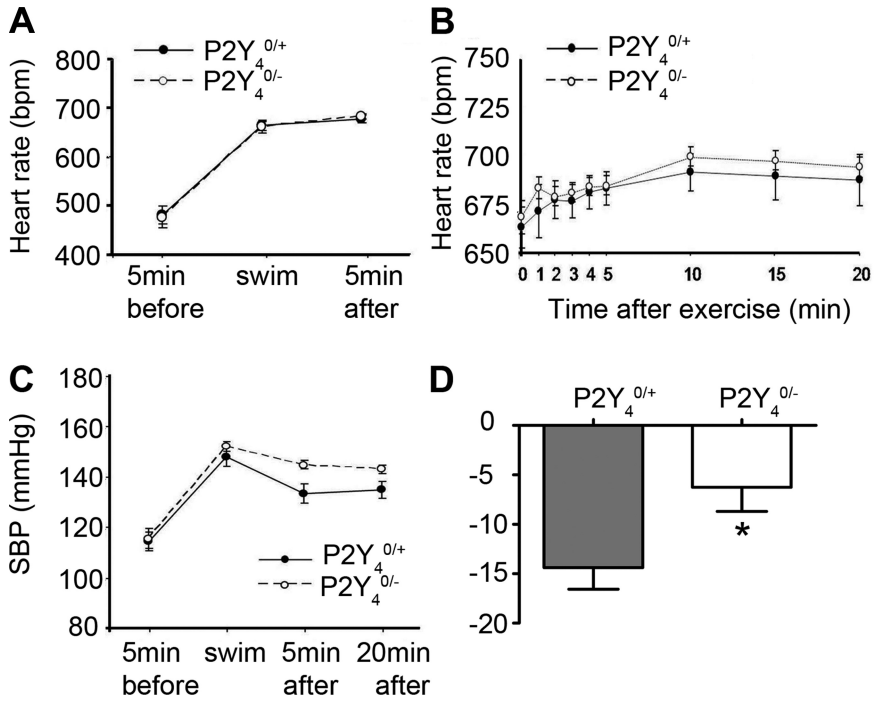

Fig. 3. Cardiac monitoring of $P2Y_4^{0/+}$ and $P2Y_4^{0/-}$ mice during swimming test. Implants have been placed in 7 $P2Y_4^{0/+}$ and 7 $P2Y_4^{0/-}$ mice. Heart rate [HR, in beats/min (bpm)] and blood pressure values have been measured in exercise conditions. HR has been recorded during 20 min, including a 10-min swimming test (*A*) and 20 min after exercise (*B*). Systolic blood pressure (SBP) values were recorded at the same time points (*C*), and ΔSBP were measured as the ratio between SBP 5 min after exercise and SBP during swimming (*D*) (*$P <$ 0.05).

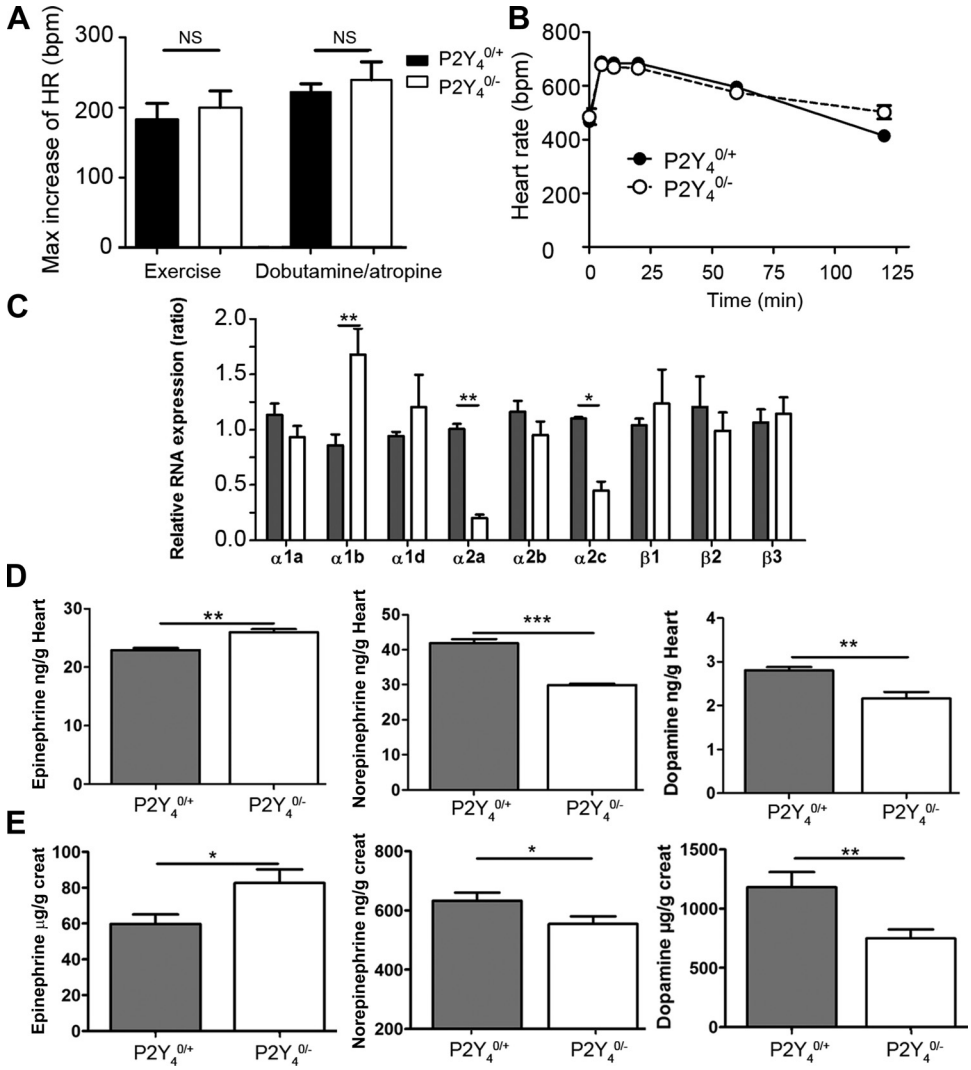

Fig. 4. *A*: comparison of HR increment induced by exercise or catecholamine challenge in $P2Y_4^{0/+}$- and $P2Y_4^{0/-}$-implanted mice. HR increment was measured in $P2Y_4^{0/+}$- and $P2Y_4^{0/-}$-implanted mice after a 10-min period of exercise or dobutamine (20 μg/g) + atropine (1 μg/g) challenge. HR was measured in conscious, unrestrained animals with surgically implanted, miniaturized telemetry devices (NS, not significant; Max, maximum). *B*: catecholamine response in $P2Y_4^{0/+}$- and $P2Y_4^{0/-}$-implanted mice. $P2Y_4^{0/+}$- and $P2Y_4^{0/-}$-implanted mice were injected with dobutamine (20 μg/g) + atropine (1 μg/g). The recording of HR was performed 25, 50, 75, 100, and 125 min after injection. *C*: adrenergic receptor quantification in $P2Y_4^{0/+}$ and $P2Y_4^{0/-}$ hearts. Total RNAs were extracted from total heart of $P2Y_4^{0/+}$ and $P2Y_4^{0/-}$ mice and reverse transcribed using Superscript II Reverse Transcriptase. Quantitative PCR were performed using specific primers for adrenergic receptors (α_{1a}, α_{1b}, α_{1d}, α_{2a}, α_{2b}, α_{2c}, β_1, β_2, and β_3). Ribosomal protein L13 (RPL13) and hypoxanthine phosphoribosyltransferase (HPRT) control genes were selected for their stability after analysis using Genorm program. Each assay was performed in duplicate for at least 2 independent preparations of heart. PCR data were normalized for each gene to RPL13 and HPRT housekeeping genes. *D*: catecholamine level in $P2Y_4^{0/+}$ and $P2Y_4^{0/-}$ hearts. Hearts of $P2Y_4^{0/+}$ and $P2Y_4^{0/-}$ 12-wk-old mice were harvested and homogenized to measure norepinephrine, epinephrine, and dopamine levels, using 3-CAT research ELISA, which were normalized to heart weight. *E*: catecholamine urine level in $P2Y_4^{0/+}$ and $P2Y_4^{0/-}$ mice. Urine samples (24 h) were collected from $P2Y_4^{0/+}$ and $P2Y_4^{0/-}$ mice to assess catecholamine levels. Urinary epinephrine, norepinephrine, and dopamine levels were measured by HPLC by electrochemical detection. Creat, creatinine. Results represent means ± SE for 19 $P2Y_4^{0/+}$ and 21 $P2Y_4^{0/-}$ mice.

plus atropine induced similar HR increment in $P2Y_4$ WT and $P2Y_4$ KO mice. Similar responses were observed in $P2Y_4$ WT and $P2Y_4$ KO mice at different times following injection (Fig. 4*B*).

We then quantified myocardial adrenergic receptor levels (Fig. 4*C*) and catecholamine levels (Fig. 4*D*) in $P2Y_4$ WT and $P2Y_4$ KO hearts. The level of α_{1a}-, α_{1b}-, α_{1d}-, α_{2a}-, α_{2b}-, α_{2c}-, β_1-, β_2-, and β_3-adrenergic receptors was quantified by quantitative PCR experiments using RNAs extracted from $P2Y_4$ WT and $P2Y_4$ KO whole hearts (Fig. 4*C*). No difference in expression was observed for β-adrenergic receptors (Fig. 4*C*). However, we observed a reduction of α_{2a}- and α_{2c}-receptor expression and an increase in α_{1b}-expression in $P2Y_4$ KO hearts compared with $P2Y_4$ WT hearts (Fig. 4*C*). Quantification of cardiac and urine level of catecholamines has provided comparable data in Fig. 4, *D* and *E*, respectively: norepinephrine and dopamine levels were reduced, whereas epinephrine level was increased in $P2Y_4$ KO mice compared with $P2Y_4$ WT mice. More precisely, the urinary content of epinephrine (60 ± 5 vs. 83 ± 7 μg/g creatinine; mean ± SE; $^*P < 0.05$; F ratio, 2.18) was higher in $P2Y_4^{0/-}$ mice, whereas those of norepinephrine (632.9 ± 27 vs. 554 ± 25 μg/g creatinine; mean ± SE; $^*P < 0.05$; F ratio, 1.02) and dopamine (1,181 ± 129 vs. 748.0 ± 77 μg/g

creatinine; mean ± SE; $^{**}P < 0.01$; F ratio, 2.54) were decreased in $P2Y_4^{0/-}$ mice compared with $P2Y_4^{0/+}$ mice (Fig. 4*E*).

Reduced Cardiac Sympathetic Innervation and Decreased Response to Hypothermia in $P2Y_4^{0/-}$ Mice

The decreased level of norepinephrine and expression of α_{2a}- and α_{2c}-receptors could be explained by a reduced sympathetic innervation of the heart. We have quantified cardiac sympathetic innervation by β-tyrosine hydroxylase staining of $P2Y_4^{0/+}$ and $P2Y_4^{0/-}$ hearts (Fig. 5, *A* and *B*). We observed a significant reduction of β-tyrosine hydroxylase staining in $P2Y_4^{0/-}$ hearts compared with $P2Y_4^{0/+}$ hearts (Fig. *5B*; $P < 0.05$).

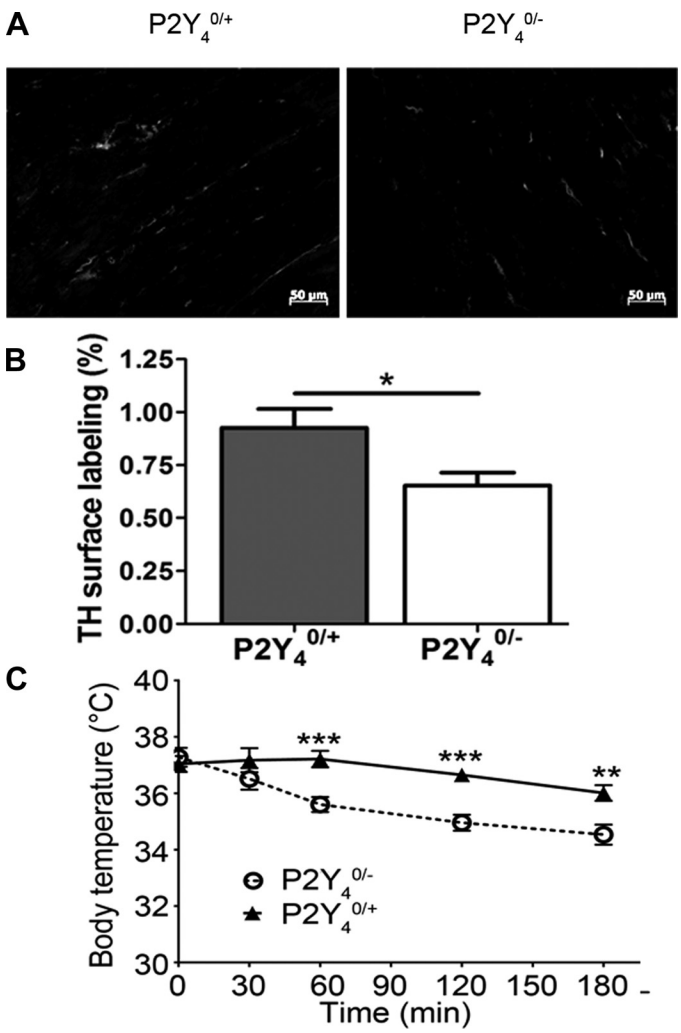

Fig. 5. Reduced cardiac innervation and decreased response to hypothermia of $P2Y_4^{0/+}$ and $P2Y_4^{0/-}$ mice. *A* and *B*: β-tyrosine hydroxylase (TH) staining of $P2Y_4^{0/+}$ and $P2Y_4^{0/-}$ hearts. Analysis of β-TH immunofluorescent staining was performed on left ventricular posterior wall to quantify sympathetic nerve fibers. Heart sections of 7 $P2Y_4^{0/+}$ and 7 $P2Y_4^{0/-}$ mice were used for anti-TH staining. The surface labeled with anti-TH antibody was measured using ImageJ software. The labeled nerve fibers was qualitatively estimated from 10 randomly selected fields and expressed as the ratio of labeled nerve fiber area to total area ($^{*}P < 0.05$). *C*: response of $P2Y_4^{0/+}$ and $P2Y_4^{0/-}$ mice to hypothermy. $P2Y_4^{0/+}$ and $P2Y_4^{0/-}$ mice were placed in a cold room at 4°C. Body temperature was measured at different periods of time from 0 to 3 h. Results are shown as means ± SE ($N = 9$) ($^{**}P < 0.01$; $^{***}P < 0.001$).

We also evaluated the response to hypothermia of $P2Y_4^{0/+}$ and $P2Y_4^{0/-}$ mice. During cold exposure, the body temperature of $P2Y_4^{0/-}$ mice decreased more rapidly than that of $P2Y_4^{0/+}$ mice (Fig. 5*C*). After 3 h, there was a difference of 1.5 ± 0.6°C between the body temperature of $P2Y_4^{0/+}$ and $P2Y_4^{0/-}$ mice (mean ± SE; $^{**}P < 0.01$; $N = 9$) (Fig. 5*C*).

Reduced Cardiac Hypertrophy in Swim-Trained P2Y4-Deficient Mice

We also investigated the effect of a prolonged effort on heart size of $P2Y_4^{0/+}$ and $P2Y_4^{0/-}$ adult mice (Fig. 6). The mice have been forced to swim two periods of 90 min per day during 3 wk. We observed a significant increase in heart size that was significantly higher in $P2Y_4^{0/+}$ mice compared with $P2Y_4^{0/-}$ mice (29 ± 6 vs. 16 ± 4%) (Fig. 6*A*). Cardiac microvascular density was evaluated in mice subjected to repeated swimming exercise (Fig. 6, *B* and *D*). Swim-trained $P2Y_4$ WT mice but not $P2Y_4$-null mice displayed a significant increase in microvessel/cardiomyocyte ratio compared with control mice (Fig. 6*B*). Cardiomyocyte size was higher in control $P2Y_4$-null mice compared with $P2Y_4$ WT mice (Fig. 6, *C* and *D*). Cardiomyocyte size was significantly increased after training in $P2Y_4$ WT mice but not in $P2Y_4$-null mice (Fig. 6, *C* and *D*).

DISCUSSION

$P2Y_4$-null mice display a defective cardiac postnatal development related to a cardiac angiogenic defect and resulting in a decreased heart weight at adult age (11). Here a combination of cardiac monitoring and exercise tests demonstrated that $P2Y_4$-null mice displayed a lower exercise capacity, a defective BP recovery after exercise, and a reduced exercise-induced cardiac hypertrophy.

More precisely, $P2Y_4$-null mice displayed reduced exercise tolerance in our two described exercise models, allowing estimation of exhaustion: motorized treadmill tests with a mild motivational shock bar and swimming tests. These results cannot be attributed to an interference with stress, locomotion, or motivational factors since the open field, black and white box, and tail suspension tests did not reveal any difference between $P2Y_4$ WT and KO mice.

A defect in the sympathetic system was suggested by the lower capacity of $P2Y_4$-deficient mice to control their body temperature under hypothermic conditions and the lower urinary norepinephrine level. However, the HR showed normal evolution in swimming mice and dobutamine plus atropine-injected mice equipped with a telemetric implant. This was consistent with the comparable expression of β_1- and β_2-receptors in the heart of $P2Y_4$-null and WT mice. Furthermore, it is known that β_1- and double β_1/β_2-receptor KO mice exhibit normal performance during exercise despite a reduced increase in HR and contractility (22, 23).

The reduced exercise capacity of $P2Y_4^{0/-}$ mice could be explained by the reduced microvascular density, which results in a failure to adequately increase blood flow and oxygen supply during exercise. Purinergic receptor activation in capillary endothelial cells by nucleotides released from hypoxic erythrocytes would initiate a retrograde vasodilator signal to the upstream arteriole (1). Furthermore, nucleotides can be released from cardiomyocytes in response to mechanical stretch (18) or during myocardial ischemia (27). We have

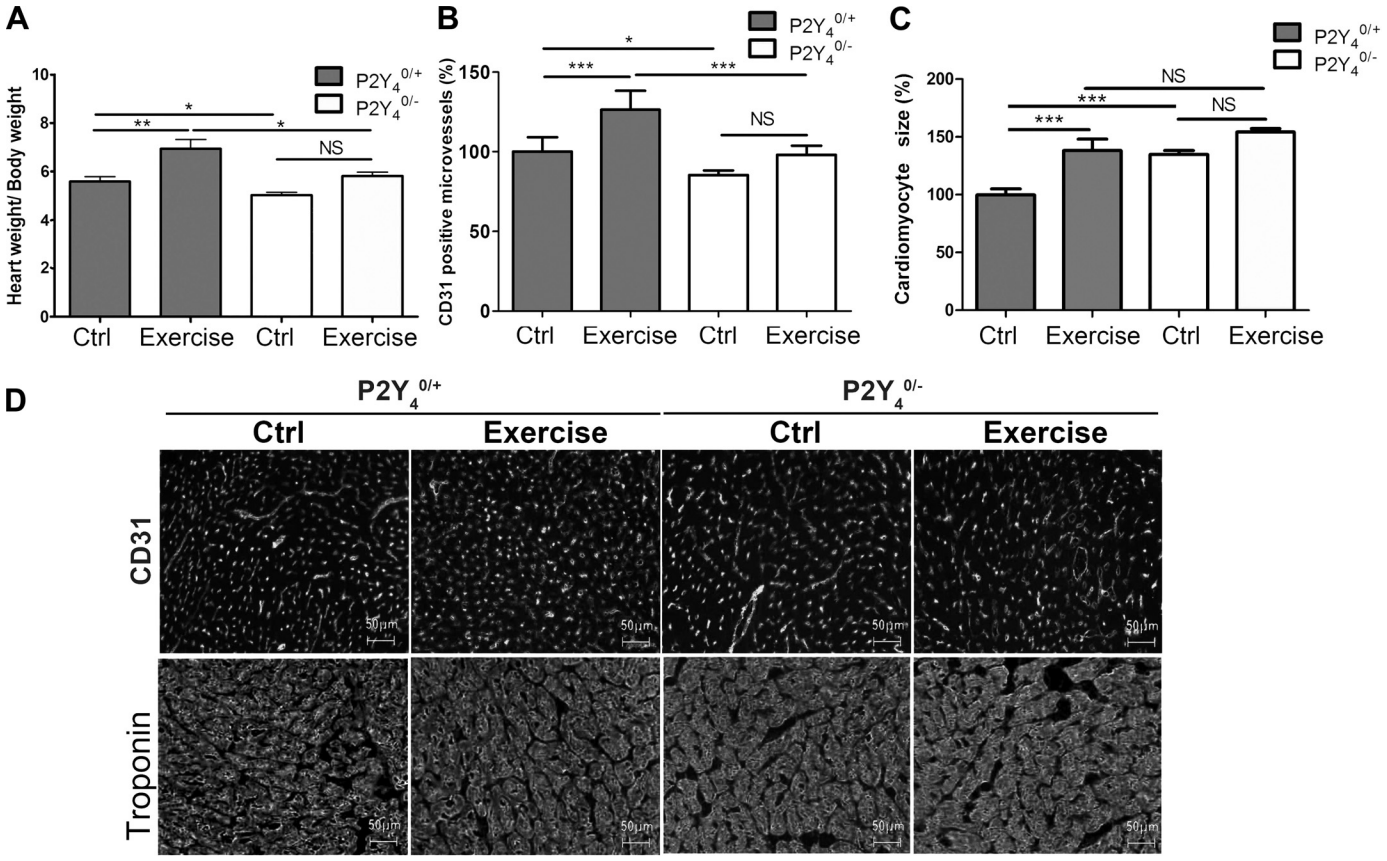

Fig. 6. Cardiac hypertrophy in swim-trained P2Y4-null mice. *A*: cardiac hypertrophy of $P2Y_4^{0/+}$ and $P2Y_4^{0/-}$ mice in response to repeated swimming tests. Swim-trained P2Y4-deficient mice show attenuated hypertrophy after 3 wk of repeated swimming tests (90 min; 2 times/day). Heart weight-to-body weight ratio has been obtained in 2 independent experiments. The results are means ± SE of 12 $P2Y_4^{0/+}$ and 14 $P2Y_4^{0/-}$ hearts from adult mice. Ctrl, control. *B*: cardiac microvascular density in $P2Y_4^{0/+}$ and $P2Y_4^{0/-}$ mice subjected to repeated swimming. Swim-trained P2Y4 wild-type mice but not P2Y4-null mice display a significant increase in microvessel-to-cardiomyocyte ratio compared with control mice. The results were blindly counted at ×20 magnification in 15 fields on transversal sections, covering at least 40% of the heart. The results are means ± SE of 8 $P2Y_4^{0/+}$ and 8 $P2Y_4^{0/-}$ hearts from adult mice. *C*: cardiomyocyte size in $P2Y_4^{0/+}$ and $P2Y_4^{0/-}$ mice in response to repeated swimming. Swim-trained P2Y4 wild-type mice show a significant increase in cardiomyocyte size compared with control mice. Cardiomyocyte size was higher in control P2Y4-null mice compared with P2Y4 wild-type mice and not significantly increased after exercise. Cardiomyocyte size has been obtained in 2 independent experiments. The results are means ± SE of 8 $P2Y_4^{0/+}$ and 8 $P2Y_4^{0/-}$ hearts from adult mice. *D*: immunofluorescent detection of CD31 and troponin in hearts of $P2Y_4^{0/+}$ and $P2Y_4^{0/-}$ mice subjected to repeated swimming. Microscopic analysis of CD31 or troponin staining at ×20 magnification in control and swim-trained $P2Y_4^{0/+}$ and $P2Y_4^{0/-}$ mice. $*P < 0.05$; $**P < 0.01$; $***P < 0.001$.

previously shown that P2Y4 receptor plays a major role in cardiac microvascular endothelial cell functions (11). In addition, a decreased cardiac output during intense exercise, related to the small size of the heart, might also play a role as reported in the case of the $\alpha_{1A/C}$-α_{1B} double KO mice (19).

Lower exercise capacity of $P2Y_4^{0/-}$ mice was identified using running and swimming tests, but cardiac monitoring was exclusively performed during swimming tests because telemetry was technically incompatible with motorized treadmill device. We observed that the postexercise recovery of SBP was delayed in the P2Y4-null mice. Interestingly, abnormal postexercise SBP was reported to be related to the extent of exercise-induced impairment of left ventricular function in patients with coronary artery disease or chronic heart failure (14, 17).

During exercise, released ATP and UTP could act on cardiomyocytes expressing $P2Y_2$ receptors and on endothelial $P2Y_2$ and P2Y4 receptors to regulate many components of the cardiac response to effort. We previously observed lower PDGF-B serum levels in P2Y4-null mice (11). PDGF-B deficiency was related to cardiac disorders including myocardial hypotrophy and septal abnormalities (2). Noteworthy, a negative effect of PDGF-B on SBP has been previously described in rats (13). Higher SBP observed in P2Y4-null mice after exercise could be correlated with PDGF-B-defective regulation.

Interestingly, the angiogenic defect associated to the loss of P2Y4 expression led to a reduced heart weight increase not only during postnatal heart development but also during the heart hypertrophic response to prolonged effort. The increase of microvessel density and cardiomyocyte size observed in P2Y4 WT mice after prolonged and repeated effort was not significant in P2Y4-null mice. The lower cardiac hypertrophy in $P2Y_4^{0/-}$ mice could be related to the angiogenic defect observed in these mice. Indeed, interactions between cardiac endothelial cells and cardiomyocytes are determinant for heart growth (12), and increased angiogenesis has been shown to induce cardiac hypertrophy (24). The loss of endothelial P2Y4 receptor that affects postnatal heart growth could thus also reduce exercise-induced cardiac hypertrophy.

In summary, reduced exercise capacity in P2Y4-null mice could result from a complex mechanism involving the various defects observed in P2Y4 KO mice, including a cardiac angio-

genic defect, a reduced norepinephrine level and sympathetic innervation of the heart, and defective BP recovery after exercise. It is likely that the decreased exercise capacity is primarily related to the smaller ventricle size and lower cardiac capillary density resulting from the altered postnatal cardiac development.

We have observed a decreased level of norepinephrine in the heart of P2Y$_4$-null mice, associated with a decreased expression of $\alpha_{2a/c}$-receptors and tyrosine hydroxylase, indicating a reduced sympathetic innervation. The exact mechanism of this defect could be complex. Norepinephrine release have been described from ATP-, UTP-, or UDP-stimulated rat sympathetic neurons, through P2X activation (3) or P2Y$_6$ activation (25). The involvement of P2Y$_4$ in catecholamine level and cardiac innervation could be an indirect consequence of heart development defect. Its importance remains unclear although it is known that $\alpha_{1A/C}$-α_{1B}-double KO mice have reduced exercise capacity (19).

In conclusion, we performed a combination of cardiac monitoring and a series of exercise, stress, and locomotion tests using our P2Y$_4$-null mice. These mice displayed decreased exercise capacity, defective BP recovery after exercise, reduced cardiac sympathetic innervation, and reduced exercise-induced cardiac hypertrophy. Our study demonstrates the involvement of a nucleotide receptor in both the acute and chronic response to exercise.

ACKNOWLEDGMENTS

We thank Dominique Fokan, Larissa di Pietrantonio, Hrag Esfahani, Laurane De Mot, and Steven Droogmans for help and technical assistance. We are grateful to Dr Andreas Markl for invaluable assistance in telemetry and helpful discussion.

GRANTS

This work was supported by an Action de Recherche Concertée of the Communauté Française de Belgique, an Interuniversity Attraction Pole grant from the Politique Scientifique Fédérale (IAP-P6/30), Prime Minister's Office, Federal Service for Science, Technology and Culture, by grants of the Fonds de la Recherche Scientifique Médicale, the Fonds d'Encouragement à la Recherche, the Fonds Emile DEFAY, the Fonds de la Recherche Scientifique Médicale of Belgium, the Walloon Region (Programme d'Excellence CIBLES), and the LifeSciHealth programme of the European Community (grant LSHB-2003–503337). D. Communi and C. Dessy are Research Associate and Senior Research Associate of the Fonds National de la Recherche Scientifique, respectively. M. Horckmans is supported by the Fonds National de la Recherche Scientifique/FRIA, Belgium. Elvira Leon-Gomez is supported by a grant of the Fonds Spécial de Recherche of the Université catholique de Louvain and the Institut de Recherche expérimentale et clinique. The funders had no role in study design, data collection and analysis, decision to publish, or preparation of the manuscript.

DISCLOSURES

No conflicts of interest, financial or otherwise, are declared by the author(s).

AUTHOR CONTRIBUTIONS

M.H., C.D., and D.C. conception and design of research; M.H. and E.L.-G. performed experiments; M.H., E.L.-G., J.-L.B., J.-M.B., C.D., and D.C. analyzed data; M.H., E.L.-G., B.R., J.-L.B., J.-M.B., C.D., and D.C. interpreted results of experiments; M.H., E.L.-G., C.D., and D.C. prepared figures; M.H. and D.C. drafted manuscript; M.H., E.L.-G., B.R., J.-L.B., J.-M.B., C.D., and D.C. edited and revised manuscript; M.H., E.L.-G., B.R., J.-L.B., J.-M.B., and D.C. approved final version of manuscript.

REFERENCES

1. **Abbracchio MP, Burnstock G, Boeynaems JM, Barnard EA, Boyer JL, Kennedy C, Knight GE, Fumagalli M, Gachet C, Jacobson KA, Weisman GA.** International Union of Pharmacology LVIII: update on the P2Y G protein-coupled nucleotide receptors: from molecular mechanisms and pathophysiology to therapy. *Pharmacol Rev* 58: 281–341, 2006.
2. **Bjarnegård M, Enge M, Norlin J, Gustafsdottir S, Fredriksson S, Abramsson A, Takemoto M, Gustafsson E, Fässler R, Betsholtz C.** Endothelium-specific ablation of PDGFB leads to pericyte loss and glomerular, cardiac and placental abnormalities. *Development* 131: 1847–1857, 2004.
3. **Boehm S, Huck Illes S, P.** UTP- and ATP-triggered transmitter release from rat sympathetic neurones via separate receptors. *Br J Pharmacol* 116: 2341–2343, 1995.
4. **Bogdanov YD, Wildman SS, Clements MP, King BF, Burnstock G.** Molecular cloning and characterization of rat P2Y4 nucleotide receptor. *Br J Pharmacol* 124: 428–430, 1998.
5. **Cheung KK, Ryten M, Burnstock G.** Abundant and dynamic expression of G protein coupled P2Y receptors in mammalian development. *Dev Dyn* 228: 254–266, 2003.
6. **Cohen R, Shainberg A, Hochhauser E, Cheporko Y, Tobar A, Birk E, Pinhas L, Leipziger J, Don J, Porat E.** UTP reduces infarct size and improves mice heart function after myocardial infarct via P2Y2 receptor. *Biochem Pharmacol* 82: 1126–1133, 2011.
7. **Communi D, Pirotton S, Parmentier M, Boeynaems JM.** Cloning and functional expression of a human uridine nucleotide receptor. *J Biol Chem* 270: 30849–30852, 1995.
8. **Desjardins F, Lobysheva I, Pelat M, Gallez B, Feron O, Dessy C, Balligand JL.** Control of blood pressure variability in caveolin-1-deficient mice: role of nitric oxide identified in vivo through spectral analysis. *Cardiovasc Res* 79: 527–536, 2008.
9. **Dutta AK, Sabirov RZ, Uramoto H, Okada YR.** Role of ATP-conductive anion channel in ATP release from neonatal rat cardiomyocytes in ischaemic or hypoxic conditions. *J Physiol* 559: 799–812, 2004.
10. **Gorman MW, Rooke GA, Savage MV, Jayasekara MP, Jacobson KA, Feigl EO.** Adenine nucleotide control of coronary blood flow during exercise. *Am J Physiol Heart Circ Physiol* 299: H1981–H1989, 2010.
11. **Horckmans M, Robaye B, Léon-Gómez E, Lantz N, Unger P, Dol-Gleizes F, Cammarata D, Schaeffer P, Savi P, Gachet C, Balligand JL, Dessy C, Boeynaems JM, Communi D.** P2Y4 nucleotide receptor: a novel actor in post-natal cardiac development and function. *Angiogenesis* 15: 349–360, 2012.
12. **Hsieh PC, Davis ME, Lisowski LK, Lee RT.** Endothelial-cardiomyocyte interactions in cardiac development and repair. *Annu Rev Physiol* 68: 51–66, 2006.
13. **Ikeda M, Morita C, Mizuno M, Sada T, Koike H, Kurokawa K.** PDGF-BB decreases systolic blood pressure through an increase in macrovascular compliance in rats. *Am J Physiol Heart Circ Physiol* 273: H1719–H1726, 1997.
14. **Kitaoka H, Takata J, Furuno T, Yamasaki F, Chikamori T, Doi YL.** Delayed recovery of postexercise blood pressure in patients with chronic heart failure. *Am J Cardiol* 79: 1701–1705, 1997.
15. **Lazarowski ER, Rochelle LG, O'Neal WK, Ribeiro CM, Grubb BR, Zhang V, Harden TK,. Boucher RC.** Cloning and functional characterization of two murine uridine nucleotide receptors reveal a potential target for correcting ion transport deficiency in cystic fibrosis gallbladder. *J Pharmacol Exp Ther* 297: 43–49, 2001.
16. **Lustig KD, Shiau AK, Brake AJ, Julius D.** Expression cloning of an ATP receptor from mouse neuroblastoma cells. *Proc Natl Acad Sci USA* 90: 5113–5117, 1993.
17. **Miyahara T, Yokota M, Iwase M, Watanabe M, Matsunami T, Koide M, Saito H, Takeuchi J.** Mechanism of abnormal postexercise systolic blood pressure response and its diagnostic value in patients with coronary artery disease. *Am Heart J* 120: 40–49, 1990.
18. **Nishida M, Sato Y, Uemura A, Narita Y, Tozaki-Saitoh H, Nakaya M, Ide T, Suzuki K, Inoue K, Nagao T, Kurose H.** P2Y6 receptor-Galpha12/13 signalling in cardiomyocytes triggers pressure overload-induced cardiac fibrosis. *EMBO J* 27: 3104–3115, 2008.
19. **O'Connell TD, Ishizaka S, Nakamura A, Swigart PM, Rodrigo MC, Simpson GL, Cotecchia S, Rokosh DG, Grossman W, Foster E, Simpson PC.** The alpha(1A/C)- and alpha(1B)-adrenergic receptors are required for physiological cardiac hypertrophy in the double-knockout mouse. *J Clin Invest* 111: 1783–1791, 2003.
20. **Razani B, Wang XB, Engelman JA, Battista M, Lagaud G, Zhang XL, Kneitz B, Hou H Jr, Christ GJ, Edelmann W, Lisanti MP.** Caveolin-2-deficient mice show evidence of severe pulmonary dys-

function without disruption of caveolae. *Mol Cell* 22: 2329–2344, 2002.
21. **Robaye B, Ghanem E, Wilkin F, Fokan D, Van Driessche W, Schurmans S, Boeynaems JM, Beauwens R.** Loss of nucleotide regulation of epithelial chloride transport in the jejunum of $P2Y_4$-null mice. *Mol Pharmacol* 63: 777–783, 2003.
22. **Rohrer DK, Chruscinski A, Schauble EH, Bernstein D, Kobilka BK.** Cardiovascular and metabolic alterations in mice lacking both beta1- and beta2-adrenergic receptors. *J Biol Chem* 274: 16701–16708, 1999.
23. **Rohrer DK, Schauble EH, Desai KH, Kobilka BK, Bernstein D.** Alterations in dynamic heart rate control in the β_1-adrenergic receptor knockout mouse. *Am J Physiol Heart Circ Physiol* 274: H1184–H1193, 1998.
24. **Tirziu D, Chorianopoulos E, Moodie KL, Palac RT, Zhuang ZW, Tjwa M, Roncal C, Eriksson U, Fu Q, Elfenbein A, Hall AE, Carmeliet P, Moons L, Simons M.** Myocardial hypertrophy in the absence of external stimuli is induced by angiogenesis in mice. *J Clin Invest* 117: 3188–3197, 2007.
25. **Vartian N, Moskvina E, Scholze T, Unterberger U, Allgaier C, Boehm S.** UTP evokes noradrenaline release from rat sympathetic neurons by activation of protein kinase C. *J Neurochem* 77: 876–885, 2001.
26. **Webb TE, Henderson D, Roberts JA, Barnard EA.** Molecular cloning and characterization of the rat P2Y4 receptor. *J Neurochem* 71: 1348–1357, 1998.
27. **Wihlborg AK, Balogh J, Wang L, Borna C, Dou Y, Joshi BV, Lazarowski E, Jacobson KA, Arner A, Erlinge D.** Positive inotropic effects by uridine triphosphate (UTP) and uridine diphosphate (UDP) via P2Y2 and P2Y6 receptors on cardiomyocytes and release of UTP in man during myocardial infarction. *Circ Res* 98: 970–976, 2006.
28. **Yitzhaki S, Shainberg A, Cheporko Y, Vidne BA, Sagie A, Jacobson KA, Hochhauser E.** Uridine-5′-triphosphate (UTP) reduces infarct size and improves rat heart function after myocardial infarct. *Biochem Pharmacol* 72: 949–955, 2006.
29. **Yitzhaki S, Shneyvays V, Jacobson KA, Shainberg A.** Involvement of uracil nucleotides in protection of cardiomyocytes from hypoxic stress. *Biochem Pharmacol* 69: 1215–1123, 2005.